

A.V. Krasilnikov, M. Sasao, Y.A. Kaschuck, V.G. Kiptily, T. Nishitani,  
S.V. Popovichev , L. Bertalot and JET EFDA contributors

# Neutron and Gamma-Ray Measurement

"This document is intended for publication in the open literature. It is made available on the understanding that it may not be further circulated and extracts or references may not be published prior to publication of the original when applicable, or without the consent of the Publications Officer, EFDA, Culham Science Centre, Abingdon, Oxon, OX14 3DB, UK."

"Enquiries about Copyright and reproduction should be addressed to the Publications Officer, EFDA, Culham Science Centre, Abingdon, Oxon, OX14 3DB, UK."

# Neutron and Gamma-Ray Measurement

A.V. Krasilnikov<sup>1,3</sup>, M. Sasao<sup>2</sup>, Y.A. Kaschuck<sup>3</sup>, V.G. Kiptily<sup>4</sup>, T. Nishitani<sup>5</sup>,  
S.V. Popovichev<sup>4</sup>, L. Bertalot<sup>6</sup> and JET EFDA contributors\*

*JET-EFDA, Culham Science Centre, OX14 3DB, Abingdon, UK*

<sup>1</sup>*RRC “Kurchatov Institute”, Academician Kurchatov square1, Moscow, 123182, Russia*

<sup>2</sup>*Tohoku University, Sendai, Japan;*

<sup>3</sup>*SRC RF TRINITI, Troitsk, 142190, Russia;*

<sup>4</sup>*EURATOM-UKAEA Fusion Association, Culham Science Centre, OX14 3DB, Abingdon, OXON, UK*

<sup>5</sup>*Japan Atomic Energy Agency, Tokai, Japan*

<sup>6</sup>*ITER Organization, Cadarach, France Italy*

*\* See annex of M.L. Watkins et al, “Overview of JET Results ”,  
(Proc. 21<sup>st</sup> IAEA Fusion Energy Conference, Chengdu, China (2006)).*

Preprint of Paper to be submitted for publication in Proceedings of the  
International Workshop on Burning Plasma Diagnostics, Villa Monastero, Varenna, Italy.  
( 24th September 2007 - 28th September 2007)



## ABSTRACT.

Due to high neutron and gamma-ray yields and large size plasmas many future fusion reactor plasma parameters such as fusion power, fusion power density, ion temperature, fuel mixture, fast ion energy and spatial distributions can be well measured by various fusion product diagnostics. Neutron diagnostics provide information on fusion reaction rate, which indicates how close is the plasma to the ultimate goal of nuclear fusion and fusion power distribution in the plasma core, which is crucial for optimization of plasma breakeven and burn. Depending on the plasma conditions neutron and gamma-ray diagnostics can provide important information, namely about dynamics of fast ion energy and spatial distributions during neutral beam injection, ion cyclotron heating and generated by fast ions MHD instabilities. The influence of the fast particle population on the 2-D neutron source profile was clearly demonstrated in JET experiments. 2-D neutron and gamma-ray source measurements could be important for driven plasma heating profile optimization in fusion reactors. To meet the measurement requirements in ITER the planned set of neutron and gamma ray diagnostics includes radial and vertical neutron and gamma cameras, neutron flux monitors, neutron activation systems and neutron spectrometers. The necessity of using massive radiation shielding strongly influences the diagnostic designs in fusion reactor, determines angular fields of view of neutron and gamma-ray cameras and spectrometers and gives rise to unavoidable difficulties in the absolute calibration. The development, testing in existing tokomaks and a possible engineering integration of neutron and gamma-ray diagnostic systems into ITER are presented.

## 1. FUSION REACTIONS AND NEUTRON SPECTRUM

### 1.1. CROSS-SECTIONS AND REACTIVITY OF FUSION REACTIONS

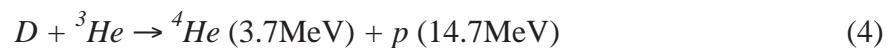
Neutrons and charged fusion products are born in D-T fusion reaction



acting as an energy source of self-sustain “burning DT plasma”, in D-D fusion reactions:



and in the D- ${}^3\text{He}$  fusion reaction:



Cross-sections of these reactions are determined by tunneling probability through a potential barrier, composed by a repulsive long-range Coulomb potential and an attractive short-range nuclear

potential. All these cross-sections have been measured experimentally down to the 10keV [1]. According to ref. [2] the cross-section energy dependence can be described by equation (5) using introduced there parameters:

$$\sigma(E) = \frac{S(E)}{E} \exp(b/E^{0.5}) \quad (5)$$

$$S(E) = \frac{A_1 + E(A_2 + E(A_3 + E(A_4 + A_5)))}{1 + E(B_1 + E(B_2 + E(B_3 + EB_4)))}$$

The fusion reactivity is the product of the cross-section and the relative velocity averaged over the Maxwellian distribution and can be parameterized as a function of the ion temperature [2]:

$$\langle \sigma v \rangle = C_1 \theta \sqrt{\frac{\xi}{m_r c^2 T^3}} e^{-3\xi} \quad (6)$$

$$\theta = T \left[ 1 - \frac{T(C_2 + T(C_4 + TC_6))}{1 + T(C_3 + T(C_5 + TC_7))} \right], \xi = \left( \frac{B_G^2}{4\theta} \right)^{1/3}, B_G = \pi \alpha Z_1 Z_2 \sqrt{2m_r c}$$

where  $B_G$  is the Gamov constant [3] and  $m_r c^2$  is the reduced mass of the particles.

## 1.2. THERMAL AND SUPER-THERMAL NEUTRON COMPONENTS

Very often the plasma contains super-thermal energetic ions originating from Neutral Beam Injection (NBI) or accelerated by Ion Cyclotron Range of Frequency (ICRF) waves. In such a case, the actual reaction rate in a plasma of a unit volume,  $Y_{total}(t)$ , is comprised of three terms: a thermal term,  $Y_{th}(t)$ , a beam thermal term,  $Y_{b-th}(t)$ , and a beam-beam term,  $Y_{b-b}(t)$ ,

$$Y_{Total} = Y_{th} + Y_{b-th} + Y_{b-b}$$

$$Y_{th} = n_i n_j \langle \sigma v \rangle_{T_i}, Y_{b-th} = n_b n_i \langle \sigma v \rangle_{b-th}, Y_{b-b} = \frac{1}{2} n_b^2 \langle \sigma v \rangle_{b-b} \quad (7)$$

$$\langle \sigma v \rangle_{12} = \iint f_1(\vec{v}_1) f_2(\vec{v}_2) \sigma(v_{rel}) v_{rel} d\vec{v}_1 d\vec{v}_2, v_{rel} = v_1 - v_2$$

Here,  $n_i(n_j)$  and  $n_b$  denote the ion density of the i-th (j-th) species, and the beam particle density, and suffixes 1 and 2 in denote either thermal or beam particles, respectively.

In many today's DD and DT plasma experiments due to the increase of reaction cross-section with energy the dominant term in (7) is the beam-thermal term,  $Y_{b-th}$ , even if the density of beam particles,  $n_b$ , is much smaller than  $n_i$ . Thus, the measurements of fusion neutron rate, neutron source profile and neutron energy distributions in present plasmas and at least in part of ITER experiments provide the information about fast ion behavior. This is in particular important for the energetic ion confinement study during: D and T NBI, ICRF heating at deuterium or tritium resonant frequencies

and “triton burn-up”, which measures the DT reaction rate produced by confined/ decelerated tritons originating from DD fusion reactions in deuterium plasma.

## **2. NEUTRON AND $\gamma$ -RAY DIAGNOSTIC MISSION**

Neutron diagnostics [4] provide information about fusion reaction rate, which indicates how close the plasma is to the ignition and burning required for making a power plant based on nuclear fusion. The neutron emission rate, which is directly related to the fusion power, can be determined by time-resolved emission monitors, which must be well calibrated in-situ, with support by activation systems and profile monitors with accuracy about 10%. The time-resolved neutron source profiles also provide useful information for transport analysis. The integral of the neutron rate from a shot is checked by the total yield, as measured by the activation system. Neutron diagnostics is also providing information about ion temperatures, fuel isotope ratio, fast ion behavior [5], degree of confinement, loss mechanism, *etc.* Velocity distributions and confinement properties of fast ions can be obtained from the neutron spectrometers and gamma ray measurement. The combination of several neutron measurement systems will provide the absolute fusion output and neutron fluence on the first wall. Fast time-resolved neutron emission rate and source profile measurements will play important roles in researches on self-heating burning plasma physics, and hence in the burning control of the device.

### **2.1. THE TIME-RESOLVED NEUTRON EMISSION RATE MEASUREMENTS**

The neutron emission rate will be used as a feedback parameter for fusion output control in ITER and future fusion reactor (neutron emission rate of 1 s<sup>-1</sup> is equivalent to the fusion power of  $1.06 \times 10^{-12}$  W in the D-T plasma and  $0.44 \times 10^{-12}$  W in the D-D plasma). Feedback control by the neutron emission rate has been demonstrated for optimization of operation, such as avoidance of minor disruptions in JT-60U [6]. Neutron emission rate diagnostics have been employed for: real-time control in JET [7] and plasma control in TFTR [8].

Detectors must have a wide dynamic range, fast response time and be not sensitive to hard X-rays and  $\gamma$ -rays. BF<sub>3</sub> and <sup>3</sup>He proportional counters, <sup>235</sup>U and threshold <sup>238</sup>U fission chambers are the most commonly used neutron detectors having time response ~100ns. Fission chambers operate in counting, Campbell and current modes. Semiconductor Si [9] and Natural Diamond (NDD) [10,11] detectors are also successfully used in counting mode for neutron flux monitoring in TFTR, JET (see Fig.1) and JT-60U. 14 MeV neutron detector based on scintillating fibers [12] was used for time-resolved triton burn-up measurements at JT-60U.

Absolute calibration is the most important problem in neutron emission rate measurements. This calibration is complicated because the neutron source is distributed in the plasma surrounded by many massive and complicated structures. Essential efforts have been devoted to absolute neutron calibrations at many tokamaks. The calibration has been performed by moving a neutron source along the known positions inside of the tokamak vacuum vessel. For absolute calibration of neutron measurements of JET and JT-60U deuterium plasmas, a <sup>252</sup>Cf neutron source was used [6]. At JET,

later the activation technique is used for cross calibration. For calibration of the DT operation in TFTR a compact DT neutron generator was used [13].

## 2.2. NEUTRON ACTIVATION MEASUREMENT

The neutron activation technique provides robust time-integrated measurements of the total neutron yield in a wide dynamic range. This enables accurate absolute calibration of fusion power and provides a flexible system for materials testing. In large tokamaks such as TFTR, JET, JT-60U the neutron activation systems consist of irradiation stations placed close to plasma, the  $\gamma$ -ray counting station and pneumatic operated sample transfer systems. To determine the relation between the neutron emission rate in the whole plasma and the neutron flux at the irradiation point the neutron Monte Carlo calculation with precise machine modeling should be applied.

At JET there is mirror symmetry of poloidal locations of irradiation ends with respect to horizontal mid-plane to correct the vertical plasma displacement influence on the total neutron yield. Sample foils transferred to the selected irradiation end via a “carousel” switching system before a plasma shot and returns to the  $\gamma$ -ray counting station by the pneumatic transfer system after the plasma shot.

Yields of DD and DT neutrons can be measured separately using several foils with different threshold energy reactions. From the ratio of DD and DT neutron yields the estimation of d/t fuel ratio in D-T plasmas can be performed. With the application of an unfolding codes the multifoil activation technique can provide a neutron energy distribution at the irradiation point [14], e.g. for test blanket modules experiments [15].

## 2.3. NEUTRON SPECTROMETRY

Spectrum of unscattered neutrons reflects the velocity distributions of reacting ions from the cone of measurements determined by collimator. For inhomogeneous Maxwellian plasma of ion temperature  $T_i$  this results in a Gaussian-shaped neutron energy spectrum with peak energy  $E_c$ , width  $W \propto \sqrt{T_i}$  and reaction rate  $I_n \propto n_i n_j \langle \sigma v \rangle T_i$  where  $n_i$ ,  $n_j$ , and  $\langle \sigma v \rangle T_i$ , are the local ion densities and reactivity, as determined in (6), respectively.

Plasmas with essential fast ion component due to auxiliary heating by NBI or ICRH will produce neutron spectra with non-Gaussian tails and Doppler energy shift relative to  $E_c$ . Fast confined  $\alpha$ -particles can give rise to alpha knock-on neutron emission in DT plasmas with high-energy tail of the spectrum. Doppler shifts in the neutron spectrum could be also caused by rotations and anisotropy in the pitch angle distribution of the fuel populations.

Neutron spectrometry could provide measurement of the following plasma parameters: ion temperature, reaction rates  $I_n \propto n_i n_j \langle \sigma v \rangle T_i$ , fusion powers for DD and DT reaction components, fuel ion densities in the core, plasma rotations, relative densities of super-thermal ions and their energy distributions, density and shape of fusion  $\alpha$ -particle energy distribution.

Large and compact neutron spectrometers were essentially upgraded during recent years. Magnetic Proton Recoil (MPR) and Time of Flight for Optimized Rate (TOFOR) large neutron spectrometer



[19] were successfully used in JET for detail high count rate neutron spectrometry. Natural diamond [11], stilbene [21] (see Fig.2) and NE-213 [22] compact neutron spectrometers also were successfully applied for neutron spectrometry at TFTR, JT-60U, JET and Tore Supra. Reached characteristics and performances of MPR and compact neutron spectrometers presented in Table 1.

#### 2.4. $\gamma$ - RAYS MEASUREMENTS

Nuclear reaction  $\geq$ -ray diagnostic is the powerful technique used for studies of the fast ion behavior in fusion devices. The emission of intense  $\geq$ -ray lines is produced when fast ions (p, d, t,  $^3\text{He}$ , and  $^4\text{He}$ ) react either with plasma fuel ions or with main plasma impurities, such as beryllium, boron, carbon, and oxygen.

$\gamma$ -ray measurements were efficiently performed on the tokamaks Doublet-III [23], TFTR [24, 25], JET [26-28], and JT-60U [29] with the application of specially developed  $\gamma$ -ray spectrometers described in Table 2.

Intensity and 2-D source profile of  $\gamma$ -rays from the  $^9\text{Be}(^3\text{He},n\gamma)^{11}\text{C}$ ,  $^9\text{Be}(^3\text{He},p\gamma)^{11}\text{B}$  and  $^{12}\text{C}(^3\text{He},p\gamma)^{14}\text{N}$  reactions are using in JET as an indicator of the efficiency and spatial distribution of ICRF power deposition in  $^3\text{He}$ -minority heating scheme [30,31].

To identify the existence in plasma the fusion  $\pm$ -particles with energies higher 1.7 and 4MeV the measurements 4.44 and 3.21MeV  $\gamma$ -rays from threshold reaction  $^9\text{Be}(\pm,n\gamma)^{12}\text{C}$  were performed [32] during and after 110keV tritium NBI.

The influence of monotonic and non-monotonic q profiles onto 2 MeV  $^4\text{He}$  ions injected into  $^4\text{He}$  plasma and accelerated by ICRF waves at their third harmonic was also successfully studied [33] be means of  $\gamma$ -ray tomography.

#### 2.5. NEUTRON/ $\gamma$ -RAY SOURCE PROFILE MEASUREMENTS

The neutron and  $\gamma$ -ray profile monitors are providing the measurements of the neutron and  $\gamma$ -ray emissivity over a poloidal cross-section of the plasma using line-integrated measurements performed by neutron and  $\gamma$ -ray detectors viewing the plasma along a number of lines-of-sight.

Being used inside neutron profile monitor, the compact neutron spectrometers is providing the information not only about the emissivity but also about the energy distribution of neutrons born at different magnetic surfaces of plasma. So, neutron source profile measurement is the principal method for the measurement fast deuteron and triton spatial and energy distributions, alpha-particle birth profile and ion temperature profile. Being absolutely calibrated the neutron source profile monitor could provide independent measurements of fusion power.

1D neutron source profiles were successfully measured in TFTR and JT-60U experiments. But in plasma with essential fast ion component the fusion neutron source and  $\gamma$ -ray profiles are not a functions of the magnetic surfaces due to non-uniformity of fast beam and ICRF-driven ion distributions on magnetic surfaces. In such cases as was demonstrated in varios JET experiments with NBI and ICRH (see Fig.3) the 2D neutron and  $\gamma$ -ray source profile measurements with

tomography reconstruction [17,18] are required to control the dynamics of spatial and energy distributions of fast confined ions.

### 3. NEUTRON AND $\gamma$ -RAY DIAGNOSTICS ON ITER

ITER will be the first burning plasma experiment with collective behaviour of the alpha particles and other fast and thermal ions. ITER plasma parameters, such as fusion power, power density, ion temperature, fast ion energy and spatial distributions in the plasma core, can be well measured by means of neutron diagnostics [34-36]. The necessity to use a massive radiation shielding strongly influences the diagnostic designs, determines angular fields of view of the neutron cameras and spectrometers and gives rise to unavoidable difficulties in the absolute calibration [37, 38].

Neutron diagnostic systems under consideration and development for ITER include: Radial (RNC) [39, 40] and Vertical (VNC) [41] neutron cameras, in-vessel [42, 43], ex-vessel [44-46] and divertor [45] neutron flux monitors, neutron activation systems [47-49] and neutron spectrometers [10,11,19-22,50]. Arrangement of the neutron diagnostic techniques and lines of sight of RNC and VNC in ITER is described in [36].

The necessity of 2D neutron profile measurements in ITER arises from the fact that, due to fast ion components, the neutron source profile may not be a constant on magnetic surfaces, especially during: ICRH, NBI, sawtooth oscillations, AE modes and in advanced tokamak regimes with strongly negative magnetic shear. To measure the fusion power with required accuracy the 2D neutron source measurements will be necessary in all these cases.

Fast ions studies will be especially important in ITER for: optimization of ICRH absorption profile, effective application of ICRH induced drift, ICRH optimization from the point of view the establishment of the fast ion profile best for sawtooth and TAE activities stabilization, optimization NBI heating and current drive profiles, studies of the features of fast D or T spatial redistribution during TAE, IRE, sawteeth crash and other MHD instabilities and their confinement on different magnetic surfaces, etc.

Compact neutron spectrometers (diamond [10], stilbene [21] and NE-213 [22] detectors) placed inside the collimators of the RNC and VNC will provide the measurements of ion temperature in the range  $T_i > 5\text{keV}$ , fast deuteron and triton energy distribution and poloidal rotation profiles. Besides compact neutron spectrometers NDD [51], CVD diamond [52], NE-213 [53] and threshold  $^{238}\text{U}$  fission chamber [54] flux monitors also will be used in RNC and VNC.

Neutron spectrometry using the magnetic proton recoil technique [19, 20] is also under consideration for  $n_T/n_D$  ratio, plasma toroidal rotation and fast ion energy distribution measurements. Possible approaches to neutron knock-on tail measurements, which should provide information about the confined-alpha-particle density and energy distribution, include MPR [19] and bubble chamber neutron spectrometers [50].

Dedicated  $\gamma$ -ray profile camera with similar to neutron cameras arrangement and  $^6\text{LiH}$  neutron filter could provide important information on the behavior of fusion  $\alpha$ -particles in ITER by means of spectroscopy of  $\gamma$ -rays born in reactions  $D(t,\gamma)^5\text{He}$  and  $^9\text{Be}(\alpha,n\gamma)^{12}\text{C}$  [28]. Candidate detectors are

single crystal spectrometers with heavy scintillators that allow measurement of g-rays in the energy range from 1–30MeV.

A strategy for the absolute calibration of ITER neutron diagnostics [36-38] includes: absolute calibration of all detectors at the manufacturer, calibration on site in a purpose built Neutron Test Area and several different methods of absolute *in-situ* calibration of the fusion power and power density measurements.

The first method is based on the absolute *in-situ* calibration of the most sensitive RNC, VNC and NFM detectors after their installation on ITER, using a radionuclide neutron source and a DT neutron generator having a neutron output of about  $10^{11}$  neutrons/s. The source will be moved inside the vacuum vessel in toroidal and poloidal directions. The most suitable period for in-situ calibration will be the end of hydrogen plasma phase. This method also involves a detailed MCNP analysis of the neutron fluxes and spectra in the RNC, VNC and NFM detector positions. The least sensitive detectors will be cross calibrated against more sensitive absolutely calibrated detectors using the plasma as the source.

The second method of the absolute calibration the RNC and VNC could be based on a characterization of the compact spectrometers and detailed MCNP calculations of the neutron flux and spectra in their locations. The compact spectrometers must be characterized on accelerator facilities and/or 2.5 and 14MeV neutron generators in terms of absolute efficiency and neutron response function for different neutron and gamma energies. In such a way the calibration factor can be determined for all compact spectrometers. Gamma sources, 2.5 and 14MeV neutron generators and/or AmBe n/ $\gamma$  sources should be build in the detector blocks or should be periodically applied during maintenance for energy calibration and stability control of the compact spectrometers.

Another independent method of absolute calibration of the fusion power measurements will be based on the calibration of foil activation system. The advantages of this method are the intrinsic linearity and time stability. It requires essential MCNP calculations. Using activation foil materials with a range of threshold energies will increase the confidence of the MCNP calculations.

## SUMMARY

The time-resolved neutron/g-ray emission rate, source profile, spectroscopy measurements and neutron activation techniques are commonly used on large current tokamaks. Many years experience in application of well developed measuring systems together with essential recent progress with neutron spectrometer development, digital signal processing, tomography reconstruction, MCNP modeling etc. insures efficient operation of neutron and g-ray diagnostics in ITER and other burning plasma installations.

The most of ITER neutron diagnostic systems have been selected, conceptually designed and integrated into the machine design. VNC and g-ray camera integration is in progress. Methods of neutron spectrometry for the  $n_T/n_D$  ratio and for the energy and spatial distribution of confined a-particles are under study.

The combination of neutron emission rate and 2D neutron source profile measurement with neutron spectrometry, activation measurement and careful calibration experiments will provide the absolute fusion power, neutron/a source profile, neutron fluence on the first wall and ion temperature profile measurements.

Fast time-response measurements of neutron emission rate and 2D source profile can be used for burn control of the plasma in the presence of fast ions and MHD instabilities.

## ACKNOWLEDGMENTS

This work was supported by Russian Agency of Atomic Energy, a Grant-in-Aid from the Ministry of Education, Culture, Sports, Science, and Technology of Japan, “Priority area of Advanced Burning Plasma Diagnostics” and United Kingdom Atomic Energy Authority (UKAEA) within the framework of the European Fusion Development Agreement (EFDA).

## REFERENCES

- [1]. A. Krauss et al., *Nuclear Physics.*, **A 465**, 150 (1987).
- [2]. H-B. Bosch and G.M. Jale, *Nuclear Fusion.*, 611-621 (1992).
- [3]. G. Gamov, *Z. Phys.*, **51**, 204 (1928).
- [4]. O.N. Jarvis, *Plasma Phys. Control. Fusion.*, **36**, 209 (1994).
- [5]. W. W. Heidbrink and G.J. Sadler, *Nuclear Fusion.*, **34**, 535 (1994).
- [6]. T. Nishitani, H. Takeuchi, T. Kondoh, et al., *Rev. Sci. Instrum.*, **63**, 5270 (1992).
- [7]. O. N. Jarvis, G. Sadler, P. van Bell and T. Elevant, *Rev. Sci. Instrum.*, **61**, 3172 (1990).
- [8]. H. W. Hendel, R.W. Palladino, C. W. Barnes, et al., *Rev.Sci.Instrum.*, **61**, 1900 (1990).
- [9]. S. Conroy, O.N. Jarvis, G. Sadler and G.B. Huxtable, *Nucl. Fusion.*, **28**, 2127 (1988).
- [10]. A.V. Krasilnikov 1998 *Diagnostics for Experimental Thermonuclear Fusion Reactor 2* ed P.E. Stott *et al* (New York: Plenum) p 439.
- [11]. A.V. Krasilnikov, et.al. *Nuc.r Instr. and Methods in Phys. Research A* **476**, 500 (2002).
- [12]. T. Nishitani, M. Hoek, H. Harano, et al., *Plasma Phys. Control. Fusion.*, **38**, 355 (1996)
- [13]. D.L. Jassby, C. W. Barnes, L.C. Johnson, et al., *Rev. Sci. Instrum.*, **66**, 891 (1995).
- [14]. B. Esposito et. al., *Rev. Sci. Instrum.*, **70**, 1130 (1999).
- [15]. M.J. Loughlin et. al., *Rev. Sci. Instrum.*, **70**, 1126 (1999).
- [16]. M. Pillon, M. Martone, O.N. Jarvis, and J. Kalne, *Fusion Technol.*, **15**, 1420 (1989).
- [17]. L.C. Ingesson et al., *Nucl. Fusion*, **38**, 1675 (1998).
- [18]. J. Mlynar et al., *Plasma Phys. Control. Fusion*, **45**, 169 (2003).
- [19]. L. Giacomelli, et. al., *Nuclear Fusion*, **45**, 1191 (2005).
- [20]. H. Henriksson, et. al., *Plasma Phys. Control. Fusion*, **47**, 1–23 (2005).
- [21]. Yu .A. Kaschuck *et al.*, *31st EPS PPCF Conf., London* (2004).
- [22]. L. Bertalot et al., *Proc.32nd EPS Conf. on Plasma Phys.*, Tarragona, Spain, ECA (2005)
- [23]. D.E. Newman, F.E. Cecil, *Nucl. Instrum. Methods*, **227**, 339 (1984).

- [24]. F.E. Cecil, S.S. Medley, *Nucl. Instrum. Methods*, **271**, 628 (1988).
- [25]. S.S. Medley et al., *Rev. Sci. Instrum.*, **61**, 3226 (1990) .
- [26]. G.J. Sadler, et al., *Fusion Technology*, **18**, 556 (1990).
- [27]. O. N. Jarvis et al., *Nuclear Fusion*, **36**, 1513 (1996).
- [28]. V. G. Kiptily, et.al., *Plasma Phys.Control.Fusion*, **48**, R59-R82 (2006).
- [29]. T. Kondoh et al., *J. Nucl. Mat.*, **241-243**, 564. (1997).
- [30]. V. G. Kiptily, et al., *Nuclear Fusion*, **42**, 999 (2002).
- [31]. M. J. Mantsinen et.al., *PRL*, **89**, 115004 (2002).
- [32]. V. G. Kiptily, et al.. *Physical Review Letters*, **93** 115001 (2004).
- [33]. V. G. Kiptily, et al., *Nuclear Fusion*, **45**, L21-L25 (2005).
- [34]. L.C. Johnson, *et al* 1998 *Diagnostics for Experimental Thermonuclear Fusion Reactor* 2ed P.E. Stott *et al* (New York: Plenum) p 409.
- [35]. M. Sasao,et al., *Plasma Phys.Control.Fusion.*, **46**, S107–S118 (2004).
- [36]. A.V. Krasilnikov, et al., *Nuclear Fusion.*, **45**, 1503 (2005). ed P.E. Stott *et al*
- [37]. G.J. Sadler, *et al* 1998 *Diagnostics for Experimental Thermonuclear Fusion Reactor* 2 ed. P.E. Stott *et al* (New York: Plenum) p 501
- [38]. Yu. A. Kaschuck 2003 ITER G XX ZZ 1 03-03-05 W0.1
- [39]. F.B .Marcus, *et al* 1998 *Diagnostics for Experimental Thermonuclear Fusion Reactor* 2, ed P.E. Stott *et al.* (New York: Plenum) p 419
- [40]. L. Petrizzi, *et al* 2004 Contract FU06 CT2003-00020(EFDA/02-1002)
- [41]. A.V. Krasilnikov, *et al*, *Instrum. Exp. Tech.* **47**, 5 (2004).
- [42]. T. Nishitani, *et al* 1998 *Diagnostics for Experimental Thermonuclear Fusion Reactor* 2, ed P.E. Stott *et al.* (New York: Plenum) p 491
- [43]. M. Yamauchi, *et al*, *Rev. Sci. Instrum.* **74**, 1730 (2003).
- [44]. C.W. Barnes and A. L. Roquemore, *Rev. Sci. Instrum.* **68**, 573 (1997).
- [45]. A.V. Krasilnikov, *et al.*, “Progress in the development of compact in-plug neutron camera and NFM for ITER” 5<sup>th</sup> Meeting of ITPA TGD (St Petersburg, July 2003)
- [46]. K. Asai *et al*, *Rev. Sci. Instrum.* **75**, 3537 (2005).
- [47]. C.W. Barnes, M.J. Loughlin and T. Nishitani, *Rev.Sci.Instrum.* **68**, 577 (1997).
- [48]. T. Nishitani, K. Ebisawa, S. Kasai and C. I. Walker, *Rev.Sci. Instrum.* **74**, 1735 (2003).
- [49]. Yu. A. Kaschuck *et al*, *Fusion Sci. Technol.* **43**, 1 (2003).
- [50]. R.K. Fisher, S.V.Tsurillo and V.S.Zaveryaev, *Rev. Sci.Instrum.* **68**, 1103 (1997)
- [51]. A.V. Krasilnikov *et al* 2002 *Advanced Diagnostics for Magnetic and Inertial Fusion* ed P.E. Stott *et al.* (New York: Kluwer Academic/Plenum) p 153
- [52]. M. Angelone, *et al*, *Rev. Sci. Instrum.* **76**, 013506 (2005).
- [53]. B. Esposito *et al*, *Rev. Sci. Instrum.* **75**, 3550 (2005).
- [54]. I.N. Aristov *et al*, *Instrum. Exp. Tech.* **47**, 15 (2004).

Spectrometer	Useful for Spectrometry sennsitivity, count/(n/cm <sup>2</sup> )	Energy resolution (FWHM),%	Energy range, MeV	Dimensions W H L, cm <sup>3</sup>	Physics studied at JET	Application
MPR	5x10 <sup>-5</sup>	2.5	>1	260x190x80	DT neutron spectrometry for: Ti(t) plasma toroidal rotation (t), fast ion energy (t) measurements with time resolution 50ms	JET
Natural Diamond Detector	2x10 <sup>-5</sup>	2	>12.5	Ø1.6.6x3	Same with time resolution 4.0s due to installation far (20m) from plasma	TFTR, JT-60U, JET
Stillbene (NE213)	10 <sup>-2</sup> - 10 <sup>-3</sup>	3	>1	Ø4x35	Same with time resolution 0.3s due usage slow analog electronics*	Tore-Supra JT-60U, JET

JG07.424-8c

Table 1: Characteristics and performance of neutron spectrometers

\*Method based on digital signal processors showed excellent performance in spectrum measurement with pulse shape discrimination for neutrons and gammas using NE213 and stilbene spectrometers [22]

Tokamak	Doublet-III	TFTR	JT - 60U	JET
Used $\gamma$ -ray spectrometers	<i>Nal(Tl)</i> Ø 5x5cm, 1 - 10 MeV $\gamma$ s	Liquid flouorocarbon scintillator <i>NE226</i> Ø 12.7x12.7cm up to 19 MeV $\gamma$ s	<i>Nal(Tl)</i> Ø5x5 inch 1-20 MeV $\gamma$ s	Two BGO (Ø7.5x7.5 cm, 1-28 MeV (4% en.res.) <i>Nal(Tl)</i> (vert) Ø12.5x15 cm, <sup>19</sup> CsI(Tl) photo-diodes (Ø20x15 mm) $E_{\gamma} > 0.2$ MeV

JG07.424-9c

Table 2: Characteristics of the g-ray spectrometers developed and used in fusion experiments

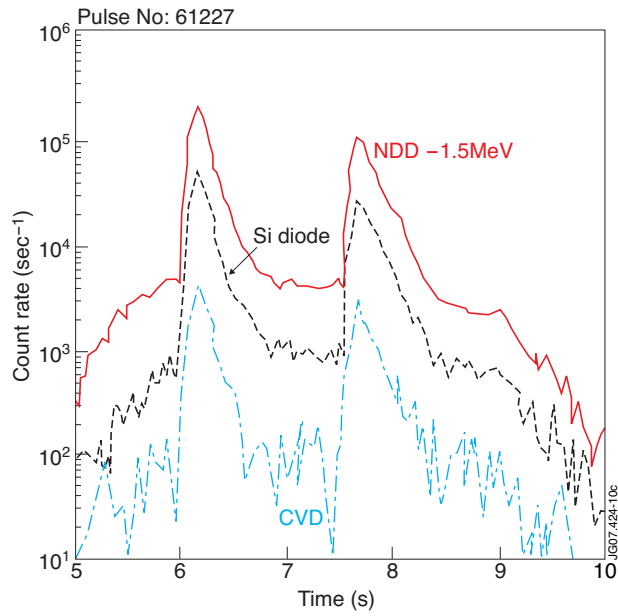


Figure 1: DT-neutron monitoring by NDD, CVD diamond and Si-diode in JET.

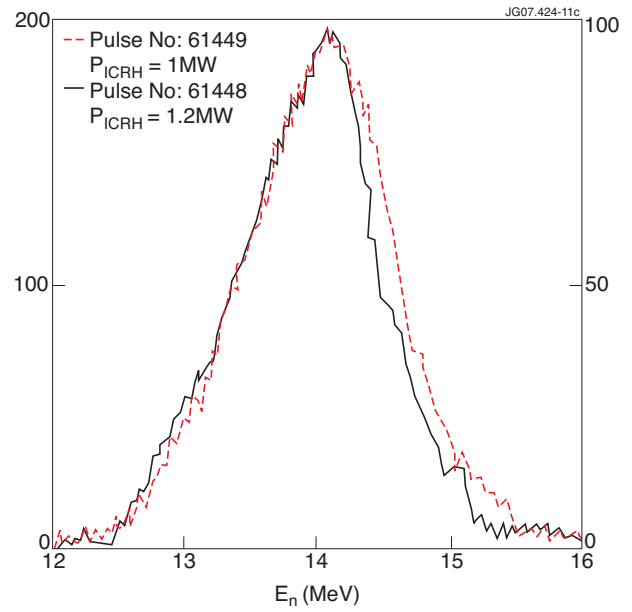


Figure 2: DT neutron spectra measured by Stilbene neutron spectrometer during T minority ICRH at JET

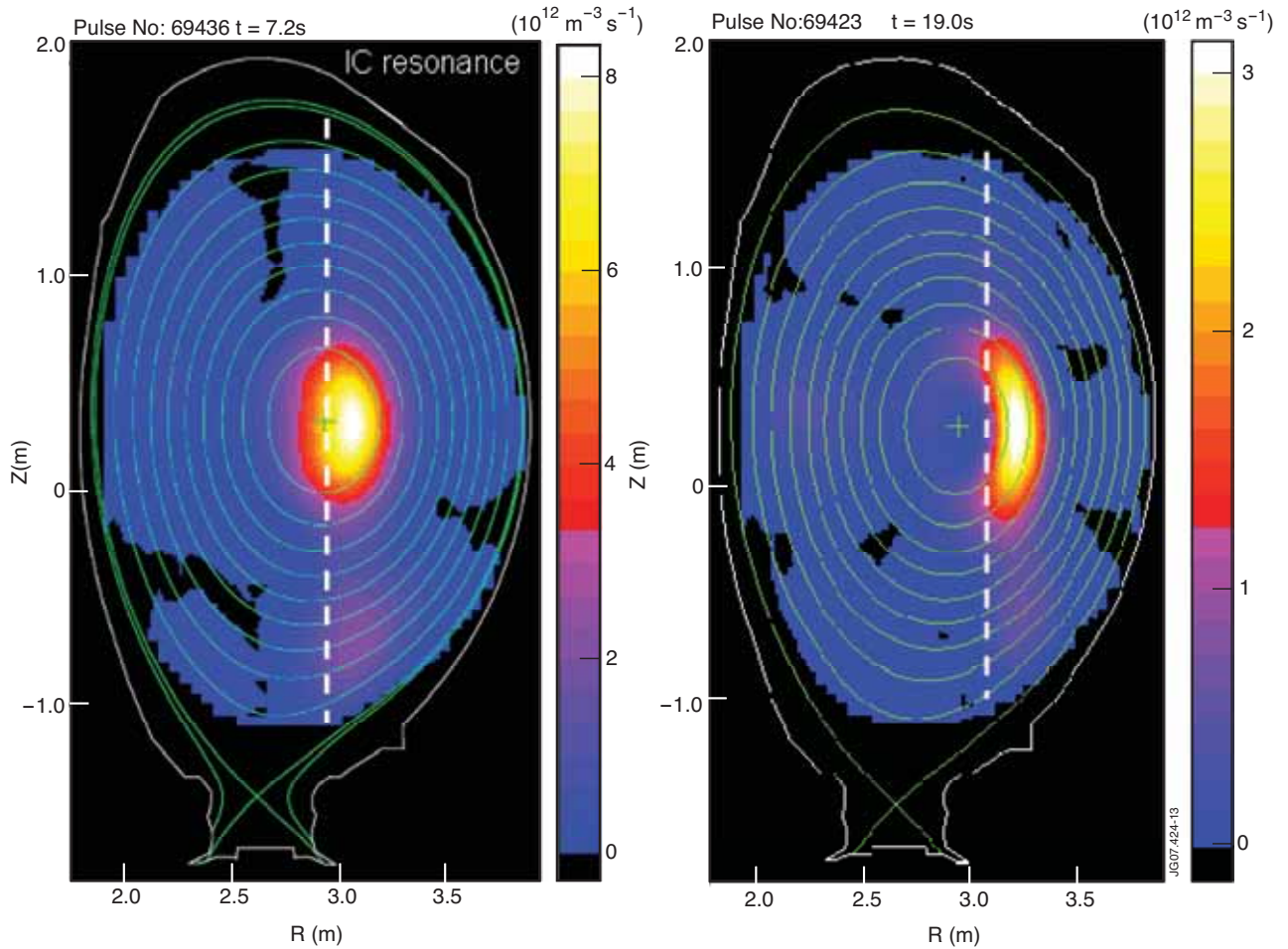


Figure 3: Tomography reconstruction of g-ray emission profiles measured in JET during  $^3\text{He}$ -minority ICRF heating discharges with central and low field side resonance layer positions